Research Article | Vol. 26, No. 11 | 28 May 2018 | OPTICS EXPRESS 14741
Optics EXPRESS

IR femtosecond pulsed laser-based fiber Bragg grating inscription in a photonic crystal fiber using a phase mask and a short focal length lens

TIGRAN BAGHDASARYAN,[1,*] THOMAS GEERNART,[1] ADRIANA MORANA,[2] EMMANUEL MARIN,[2] SYLVAIN GIRARD,[2] MARIUSZ MAKARA,[3] PAWEŁ MERGO,[3] HUGO THIENPONT,[1] AND FRANCIS BERGHMANS[1]

[1]*Vrije Universiteit Brussel (VUB), Department of Applied Physics and Photonics (TONA), Brussels Photonics (B-PHOT), Pleinlaan 2, B-1050 Brussels, Belgium*
[2]*Laboratoire Hubert Curien, Université Jean Monnet, CNRS UMR 5516, 18 Rue Prof. B. Lauras, 42000 Saint-Etienne, France*
[3]*Maria Curie-Skłodowska University, 20-031 Lublin, Poland*
[*]*tbaghdas@vub.be*

Abstract: Fiber Bragg grating inscription with infrared femtosecond pulsed lasers in photonic crystal fiber is far from being trivial due to the presence of air holes in the cladding region and the non-linear nature of the absorption process inducing the required refractive index changes. We have studied this problem numerically and experimentally for a phase mask-based writing setup equipped with short focal length cylindrical lenses, which are often used for through-coating and high temperature stable grating writing. We have shown that for a cylindrical lens with a focal length f of 10 mm, the hexagonal lattice PCF needs to be translated away from the beam waist position by around 15 µm to efficiently deliver the energy to the core region. We have also investigated the importance of the PCF's angular orientation and we have shown that for some optimal positions the same behavior is observed for cylindrical lenses with different focal lengths. Finally, we have succeeded in writing a 4 dB strong grating in a photonic crystal fiber with a 1030 nm femtosecond pulsed laser in around 4 seconds, using an acylindrical lens with f = 10 mm.

OCIS codes: (060.3735) Fiber Bragg gratings; (060.5295) Photonic crystal fibers; (140.7090) Ultrafast lasers.

References and links

1. K. O. Hill and G. Meltz, "Fiber Bragg grating technology fundamentals and overview," J. Lightwave Technol. **15**(8), 1263–1276 (1997).
2. P. Russell, "Photonic crystal fibers," Science **299**(5605), 358–362 (2003).
3. L. Thevenaz, *Advanced Fiber Optics: Concepts and Technology* (EPFL, 2011).
4. F. Berghmans, T. Geernaert, T. Baghdasaryan, and H. Thienpont, "Challenges in the fabrication of fibre Bragg gratings in silica and polymer microstructured optical fibres," Laser Photonics Rev. **8**(1), 27–52 (2014).
5. J. Thomas, C. Voigtländer, R. G. Becker, D. Richter, A. Tünnermann, and S. Nolte, "Femtosecond pulse written fiber gratings: a new avenue to integrated fiber technology," Laser Photonics Rev. **6**(6), 709–723 (2012).
6. S. J. Mihailov, D. Grobnic, C. Hnatovsky, R. B. Walker, P. Lu, D. Coulas, and H. Ding, "Extreme Environment Sensing Using Femtosecond Laser-Inscribed Fiber Bragg Gratings," Sensors (Basel) **17**(12), 2909 (2017).
7. A. Martinez, I. Y. Khrushchev, and I. Bennion, "Direct inscription of Bragg gratings in coated fibers by an infrared femtosecond laser," Opt. Lett. **31**(11), 1603–1605 (2006).
8. D. Grobnic, S. J. Mihailov, C. W. Smelser, and R. T. Ramos, "Ultrafast IR Laser Writing of Strong Bragg Gratings Through the Coating of High Ge-Doped Optical Fibers," IEEE Photonics Technol. Lett. **20**(12), 973–975 (2008).
9. D. Grobnic, C. Hnatovsky, and S. J. Mihailov, "Thermally Stable Type II FBGs Written Through Polyimide Coatings of Silica-Based Optical Fiber," IEEE Photonics Technol. Lett. **29**(21), 1780–1783 (2017).
10. A. Morana, S. Girard, E. Marin, J. Périsse, J. S. Genot, J. Kuhnhenn, J. Grelin, L. Hutter, G. Mélin, L. Lablonde, T. Robin, B. Cadier, J. R. Macé, A. Boukenter, and Y. Ouerdane, "Radiation-Hardened Fiber Bragg Grating Based Sensors for Harsh Environments," IEEE Trans. Nucl. Sci. **64**(1), 68–73 (2017).

#323170 https://doi.org/10.1364/OE.26.014741
Journal © 2018 Received 23 Feb 2018; revised 4 May 2018; accepted 16 May 2018; published 25 May 2018

Optics EXPRESS

11. G. D. Marshall, D. J. Kan, A. A. Asatryan, L. C. Botten, and M. J. Withford, "Transverse coupling to the core of a photonic crystal fiber: the photo-inscription of gratings," Opt. Express **15**(12), 7876–7887 (2007).
12. S. Pissadakis, M. Livitziis, and G. D. Tsibidis, "Investigations on the Bragg grating recording in all-silica, standard and microstructured optical fibers using 248 nm, 5 ps laser radiation," J. Eur. Opt. Soc. **4**, 09049 (2009).
13. J. Canning, "Fibre gratings and devices for sensors and lasers," Laser Photonics Rev. **2**(4), 275–289 (2008).
14. T. Baghdasaryan, T. Geernaert, F. Berghmans, and H. Thienpont, "Geometrical study of a hexagonal lattice photonic crystal fiber for efficient femtosecond laser grating inscription," Opt. Express **19**(8), 7705–7716 (2011).
15. A. V. Dostovalov, A. A. Wolf, V. K. Mezentsev, A. G. Okhrimchuk, and S. A. Babin, "Quantitative characterization of energy absorption in femtosecond laser micro-modification of fused silica," Opt. Express **23**(25), 32541–32547 (2015).
16. D. N. Nikogosyan, "Multi-photon high-excitation-energy approach to fibre grating inscription," Meas. Sci. Technol. **18**(1), R1–R29 (2007).
17. S. J. Mihailov, D. Grobnic, and C. W. Smelser, "Femtosecond IR laser fabrication of Bragg gratings in photonic crystal fibers and tapers," IEEE Photonics Technol. Lett. **18**(17), 1837–1839 (2006).
18. D. Grobnic, H. Ding, S. J. Mihailov, C. W. Smelser, and J. Broeng, "High birefringence fibre Bragg gratings written in tapered photonic crystal fibre with femtosecond IR radiation," Electron. Lett. **43**(1), 16–17 (2007).
19. T. Geernaert, K. Kalli, C. Koutsides, M. Komodromos, T. Nasilowski, W. Urbanczyk, J. Wojcik, F. Berghmans, and H. Thienpont, "Point-by-point fiber Bragg grating inscription in free-standing step-index and photonic crystal fibers using near-IR femtosecond laser," Opt. Lett. **35**(10), 1647–1649 (2010).
20. C. Wang, J. He, J. Zhang, C. Liao, Y. Wang, W. Jin, Y. Wang, and J. Wang, "Bragg gratings inscribed in selectively inflated photonic crystal fibers," Opt. Express **25**(23), 28442 (2017).
21. S. J. Mihailov, C. Hnatovsky, D. Grobnic, K. Chen, and M. J. Li, "Fabrication of bragg gratings in random air-line clad microstructured optical fiber," IEEE Photonics Technol. Lett. **30**(2), 209–212 (2018).
22. T. Baghdasaryan, T. Geernaert, H. Thienpont, and F. Berghmans, "Numerical modeling of femtosecond laser inscribed IR gratings in photonic crystal fibers," Opt. Express **23**(2), 709–723 (2015).
23. T. Baghdasaryan, T. Geernaert, H. Thienpont, and F. Berghmans, "Photonic crystal mikaelian lenses and their potential use as transverse focusing elements in microstructured fibers," IEEE Photonics J. **5**(4), 7100512 (2013).
24. T. Baghdasaryan, T. Geernaert, K. Chah, C. Caucheteur, K. Schuster, J. Kobelke, H. Thienpont, and F. Berghmans, "Anomalous transparency in photonic crystals and its application to point-by-point grating inscription in photonic crystal fibers," Sci. Rep. **8**(1), 5470 (2018).
25. J. Thomas, E. Wikszak, T. Clausnitzer, U. Fuchs, U. Zeitner, S. Nolte, and A. Tünnermann, "Inscription of fiber Bragg gratings with femtosecond pulses using a phase mask scanning technique," Appl. Phys., A Mater. Sci. Process. **86**(2), 153–157 (2006).
26. Y. Li, C. R. Liao, D. N. Wang, T. Sun, and K. T. V. Grattan, "Study of spectral and annealing properties of fiber Bragg gratings written in H2-free and H2- loaded fibers by use of femtosecond laser pulses," Opt. Express **16**(26), 21239–21247 (2008).
27. M. Bernier, S. Gagnon, and R. Vallée, "Role of the 1D optical filamentation process in the writing of first order fiber Bragg gratings with femtosecond pulses at 800nm [Invited]," Opt. Mater. Express **1**(5), 832 (2011).
28. R. Suo, J. Lousteau, H. Li, X. Jiang, K. Zhou, L. Zhang, W. N. MacPherson, H. T. Bookey, J. S. Barton, A. K. Kar, A. Jha, and I. Bennion, "Fiber Bragg gratings inscribed using 800nm femtosecond laser and a phase mask in single- and multi-core mid-IR glass fibers," Opt. Express **17**(9), 7540–7548 (2009).
29. C. W. Smelser, D. Grobnic, and S. J. Mihailov, "Generation of pure two-beam interference grating structures in an optical fiber with a femtosecond infrared source and a phase mask," Opt. Lett. **29**(15), 1730–1732 (2004).
30. Lumerical Inc, http://www.lumerical.com/tcad-products/fdtd/.
31. D. Grobnic, C. Hnatovsky, R. Lausten, and S. J. Mihailov, "Dynamics of the Fluorescence Intensity during Fiber Bragg Gratings Inscription in SMF28 and Pure Silica Core Fiber using 800 nm Fs Radiation," in *Bragg Gratings, Photosensitivity, and Poling in Glass Waveguides* (Optical Society of America, 2016), paper BTh3B–7.

1. Introduction

A fiber Bragg grating (FBG) is a periodic modification of the refractive index in the core region of an optical fiber that serves as a wavelength selective mirror [1]. The most common applications of FBGs can be found in optical fiber communications, fiber sensing and fiber lasers. Photonic crystal fibers (PCFs) [2] are also considered for such applications [3]. This prompted investigations on the inscription of FBGs in PCFs, which has developed into a research topic in its own right. In spite of the multitude of research efforts conducted so far [4], efficient inscription of FBGs using near infrared (IR) femtosecond lasers pulses in PCFs is still a challenge.

Using IR femtosecond pulses for grating writing instead of traditional ultraviolet sources eliminates the necessity for a photosensitive core region, and allows for gratings to be

Optics EXPRESS

inscribed in almost any type of transparent materials [5]. This inscription technique also delivered temperature stable (up to 1000°C) Type II FBGs in traditional step-index fibers [6] and allowed for inscription through the polymer coating [7–9]. FBGs suitable for sensing in a harsh nuclear environment were also demonstrated using IR femtosecond lasers [10].

However, when attempting to write gratings in PCFs with femtosecond pulses, the latter experience multiple interactions with the air holes in the fiber's cladding region, and only a limited amount of the laser power reaches the actual core region [11–14]. The effect of this reduced coupling efficiency is exacerbated when using IR femtosecond pulses, as the latter require multi-photon (up to 7-photons [15]) absorption to occur in order to generate refractive index changes [6,16]. The multiple interactions of the grating writing pulses with the air holes, the rotational dependence, the non-linear absorption in the cladding region, the potential filamentation of the laser writing beam, ablation at the surface of the air holes and the non-uniform distribution of the index modifications across the PCF core all contribute to lowering the efficiency of the grating writing and make grating formation in PCFs a very complex matter altogether.

So far, only a very limited number of phase mask setup-based IR femtosecond pulse gratings were fabricated in PCFs [17–21]. The first of such gratings was obtained in 2006 by Mihailov et al. in a commercial PCF that had a hexagonal lattice cladding with 4 rings of air holes using a Ti:Sapphire laser at 800 nm [17]. The authors noticed a strong rotational dependence of the grating growth, i.e. grating growth varied strongly with the angular orientation of the PCF's microstructure relative to the direction of the writing beam. In the same publication, gratings were also written in a PCF with 7 rings of air holes, however grating growth was only possible after tapering the PCF. One year later, the same group reported highly birefringent FBG inscription in another type of tapered PCF [18]. In 2017, Wang et al. reported on IR femtosecond pulse-based grating inscription in a commercially available PCF using a phase mask technique [20]. To cope with the influence of the air holes, the cladding region of the PCF was selectively inflated at the location where the FBG was meant to be inscribed. Femtosecond IR pulse laser-based gratings were also inscribed in another type of specialty optical fiber with a phase mask approach, i.e. in a so-called random air-line clad microstructured optical fiber, in which the influence of the air holes was minimal owing to the small dimensions of these randomly distributed air holes in the cladding region [21].

The fact that only a single phase mask-based IR femtosecond pulse written FBG was demonstrated in non-modified PCF, whilst other successful grating writing attempts required either tapered or inflated PCFs, points to how difficult and challenging this procedure is. This prompted us to research into understanding the role of the holey cladding, of the inscription conditions and of the highly non-linear nature of the index change in view of enabling efficient grating writing procedure. In our previous reports, we already addressed the influence of the PCF's angular orientation relative to the grating writing direction [14], the effect of the non-uniformly induced index change in the core region [22] and we even proposed dedicated PCF design with a gradient index-like photonic crystal cladding facilitating grating writing [23]. Very recently, we have also designed and fabricated a special PCF with holey cladding features that convey anomalous transparency characteristics to the photonic crystal cladding (for the given grating inscription wavelength in the IR), and we successfully inscribed a point-by-point grating therein [24].

In this manuscript, we focus on phase mask-based IR femtosecond grating inscription in a PCF for varying writing conditions and, in particular, using a cylindrical lens with a short focal length. The latter is an essential element in the phase mask setup that governs the inscription conditions. The function of this lens is to focus the laser beam on the fiber core region. From literature we learn that lenses with focal lengths from 12 mm to 30 mm and higher have been used for phase-mask-based IR femtosecond grating writing in standard step-index fibers [5,6,8–10,25–28]. Grating writing in a non-processed PCF mentioned above, for

Optics EXPRESS

example, was also carried out with a 30 mm focal length lens [17]. One is currently moving towards grating writing through the coating, i.e. without any need for stripping and re-coating the fiber at the location of the grating, using shorter focal length lenses. This allows decreasing the optical intensity in the polymer coating region, which has a much lower absorption threshold than of the fiber's silica [5–9]. Short focal length lenses also decrease the probability of damaging the phase mask, since laser pulses with lower power can be used to achieve the threshold intensities required for inducing the index change in the focal region. We therefore investigate in detail the use of a short focal length lens with f = 10 mm to write IR femtosecond gratings in hexagonal lattice PCF.

The paper is structured as follows: in the second section, we detail the grating inscription conditions, we introduce our modeling approach and we discuss the simulations of the distribution of the optical intensity in regular step-index fiber when using cylindrical lenses with different focal lengths. In Section 3, we study the influence of the PCF's angular orientation, while in Section 4 we address the alignment tolerances for cylindrical lenses with different focal lengths. Section 5 shows our experimental results and actual FBG inscription in a PCF with a f = 10 mm focal length cylindrical lens. We summarize our findings and close the paper with Section 6.

2. Modeling IR phase mask grating inscription in PCF and focusing with different cylindrical lenses

The phase mask-based inscription configuration that we have used in our experiments and that we have modeled below is illustrated in Fig. 1. The 1030 nm femtosecond pulses first pass through a cylindrical lens, which focuses the laser beam along the fiber core. A holographic phase mask (purchased from Ibsen Photonics) with a period of 2.175 μm is placed behind the lens. According to the manufacturer, the zero order diffraction efficiency is only 0.8% at 1030 nm wavelength. The fiber is positioned in the near field interference pattern formed by the + 1 and −1 diffraction orders created by the phase mask, which is optimized to feature maximal diffraction efficiency in these orders. The so-called order walk-off effect of the higher order diffracted beams, specific to femtosecond laser-based setups, helps to achieve a pure two beam interference pattern at the fiber location if the latter is placed at the correct distance from the phase mask [5,6,29]. The period of the interference pattern corresponds to that of the second order grating resonance for a wavelength of 1550 nm in a conventional single-mode step-index fiber.

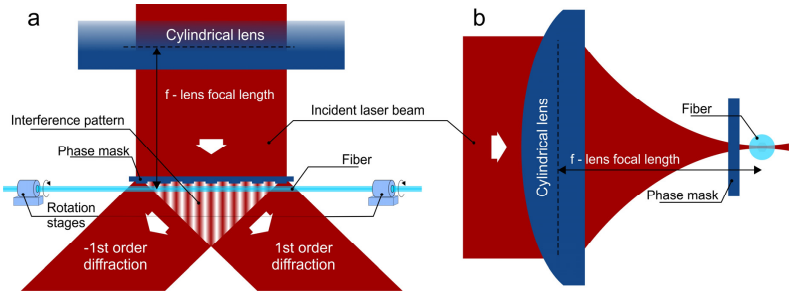

Fig. 1. Illustration of the IR phase mask grating inscription seen from two perspectives: a) near field interference from the phase mask and b) focusing using a cylindrical lens.

To understand the illumination conditions generated in such a setup, we first modeled focusing of the laser beam to the core region of a regular step-index fiber with different cylindrical lenses using finite difference time domain (FDTD) simulations. For that purpose we used the commercial FDTD Solutions software from Lumerical Inc [30]. The inscribing Gaussian beam propagates downwards along the –Y direction from the top. We looked into cylindrical lenses, see Fig. 1(b), used to focus a beam with a diameter of 4 mm directly to the center of the fiber, with focal lengths f of 10 mm, 12 mm, 19 mm and 30 mm. The last three

Optics EXPRESS

values are often encountered in literature. Figure 2 shows the normalized intensity distribution in a cross-section of a standard step-index fiber. Note that we took into account the influence of the 125 µm outer cladding region on the focusing as well as the presence of the phase mask in the setup, and that we considered that the interference pattern is formed by beams impinging under a certain angle. We have shown previously that for such 2D transverse coupling simulations, one should only consider the wave vector component in the cross-sectional plane (XY) [22]. For this particular phase mask with a period of 2.175 µm, the angle of the first order diffracted beam is around 28° and the corresponding effective wavelength is 1170 nm (calculated for the 1030 nm free space wavelength).

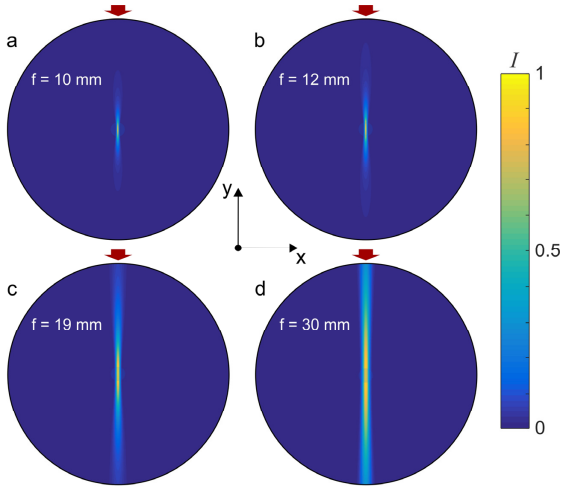

Fig. 2. Normalized intensity distributions in a standard step-index fiber. The grating writing beam is focused to the core region using cylindrical lenses with different focal lengths f.

Figure 2 reveals that the intensity distribution in the focal region and the dimensions of the focal region vary considerably when changing the cylindrical lens. Detailed data for the beam waist diameter and depth of focus, which we defined here as the full width at half maximum (FWHM) of the intensity distribution along the Y axis extracted from Fig. 2, are summarized in Table 1. For instance, for f = 30 mm, the beam waist diameter is 6.86 µm, while the depth of focus is larger than the fiber diameter. In this case, the Gaussian beam intensity close to the coating is comparable with the intensity in the core region, meaning that through-coating inscription would be nearly impossible. For f = 10 mm, however, the waist diameter decreases to 2.34 µm and the depth of focus is as small as 15.7 µm. The results for f = 10 mm also illustrate the difficulties when working with short focal length lenses. First, the overlap of the beam with the fiber core region along the X axis becomes much lower and for that reason beam scanning along the X axis with piezo elements is often practiced. Second, the alignment tolerance along the Y axis is much less than for setups with a longer focal length.

Table 1. Dimensions of the focal region for a 4 mm width Gaussian beam focused on a step-index fiber core region using cylindrical lenses with different focal lengths f.

Focal length	Waist diameter	Depth of focus
f = 10 mm	2.34 µm	15.7 µm
f = 12 mm	2.66 µm	22.3 µm
f = 19 mm	4.28 µm	56.2 µm
f = 30 mm	6.86 µm	> 125 µm

In the next two sections, we will use the illumination conditions depicted in Fig. 2 applied to a PCF in order to study the peculiarities of grating writing in holey fibers when cylindrical

Optics EXPRESS

lenses with different focal length are used. The PCF under test here has already been described in previous work and holds 6 rings of air holes organized in a hexagonal structure [14]. The fiber has been manufactured at the University Marie Curie-Skłodowska (Lublin, Poland). The scanning electron microscope image of the PCF's cross-section is shown in Fig. 3. The outer diameter is 126 µm, the air hole pitch is Λ = 3.46 µm and the air hole diameter is d = 1.36 µm, resulting in a relatively low filling factor of d/Λ = 0.39. The diameter of the core region inside the inner ring of air holes is 5.56 µm, while the ratio of the germanium doped (3.1 mol%) core diameter to the entire core diameter is 0.6. The germanium doping here is not required not support the guidance of light in the optical fiber, but will be useful for aligning the PCF in the grating writing setup owing to the fluorescence signal emitted by the germanium doped region.

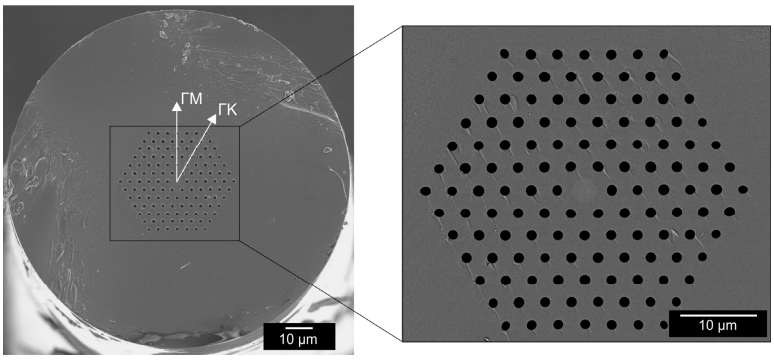

Fig. 3. Scanning electron microscope image of the PCF considered in the work.

3. Rotational dependence of the transverse coupling for different focusing conditions

It is well-known that grating writing in PCFs is 'sensitive' to the angular orientation of the microstructure with respect to the direction of the writing beam when femtosecond laser sources are used [14,17,22]. This rotational dependence is particularly pronounced at IR wavelengths, as a highly non-linear up to 7-photon absorption process is involved to create index changes.

We study this issue here for the PCF described earlier by calculating the amount of optical power reaching the core region (with a radius of 2.78 µm) when using cylindrical lenses with different focal lengths and by varying the angular orientation. As a figure of merit, we will use the transverse coupling efficiency (TCE), which is defined as the ratio of the integrated core field intensities calculated in the presence and absence of a microstructured cladding. We have introduced this TCE in previous publications and we refer to these for more detailed information on how the TCE is defined and calculated [4,14]. A TCE lower than 1 indicates that the holey cladding has a detrimental influence on the amount of inscription light that reaches the core region, while a TCE equal to or close to 1 means that the structured cladding has no influence or only a minimal effect.

Optics EXPRESS

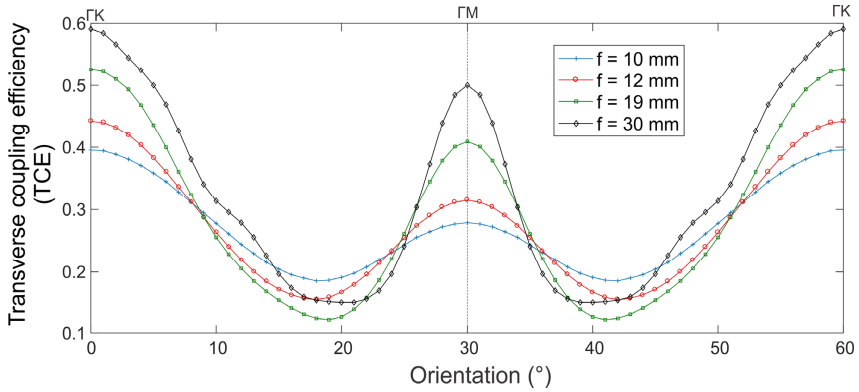

Fig. 4. TCE dependence on the PCF angular orientation for four different focal lengths. Only angles from 0 to 60° are shown for sake of symmetry of the hexagonal air hole lattice.

Figure 4 shows the rotational dependence of the TCE for four cylindrical lenses. 0° corresponds to incidence along the ΓK axis, while 30° means incidence along the ΓM axis, see Fig. 3. Extrema and average values are summarized in Table 2.

Table 2. Statistical data for the TCE dependence on the PCF angular orientation.

	TCE		
Focal length	Minimum	Maximum	Average
f = 10 mm	0.19	0.4	0.27
f = 12 mm	0.16	0.44	0.27
f = 19 mm	0.12	0.53	0.29
f = 30 mm	0.15	0.59	0.33

The optimal orientation for all cylindrical lenses is 0° (ΓK direction). We obtain a maximum TCE of 0.59 for f = 30 mm, while for the other lenses the maximum values are 0.53 for f = 19 mm, 0.44 for f = 12 mm and 0.4 for f = 10 mm. The rotational dependence is more pronounced for the longer focal lengths, whilst the averaged TCE over all the angles is quite similar for the different lenses.

4. Translational dependence of the transverse coupling for different focusing conditions

In the previous section, we have calculated the TCE for a laser beam focused to the center of the fiber core region. This corresponds to the situation shown in Fig. 2, after adding the holey microstructure to the simulations. However, and given the effect of adding the air holes, it is not trivial that this is the optimal position of the focus for grating writing. To investigate this further, we translated the PCF along the X and Y axes relative to the initial position corresponding to the focus located in the center, and we calculated the TCE for all those configurations. We fixed the orientation of the PCF such that the incidence of the grating writing beam is along the ΓK direction, since we found maximum TCE values for this particular orientation, see Fig. 4.

Optics EXPRESS

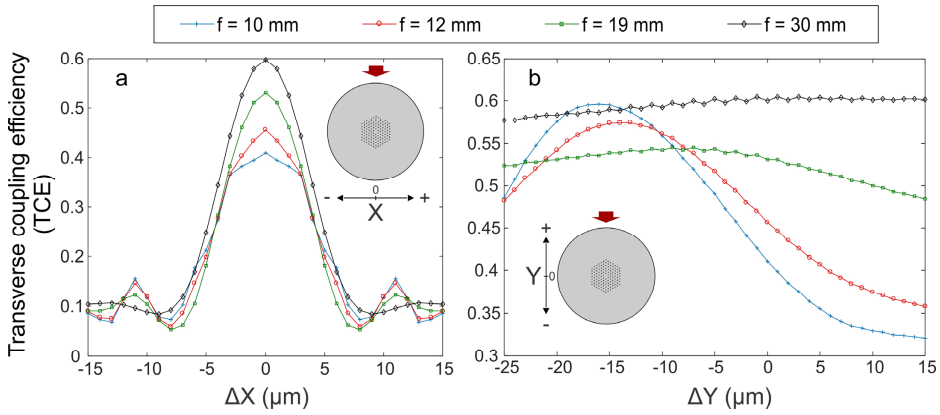

Fig. 5. Translational dependence of the TCE along a) the X axis and b) the Y axis for incidence along the ΓK for four different focal lengths.

Figure 5 shows the results. For horizontal translation along the X axis, shown in Fig. 5(a), the behavior for all four lenses is very similar, with a FWHM of the curves around 10 µm. We find a maximum TCE value for all four lenses at a translation $\Delta X = 0$, i.e. for a focus located exactly in the center of the core region. We observe only minor peculiarities in small side peaks around $\Delta X = 12$ µm and in the fact that the TCE is not 0, even for maximal translations of $\Delta X = \pm 15$ µm. The latter results from the interaction of the beam with the microstructure, which redistributes the optical energy inside the holey region and redirects some of it into the core region.

The analysis for the vertical translation along the Y axis in Fig. 5(b), i.e. along the direction of the incident laser beam, reveals much more interesting results. For long focal length lenses, with f = 30 mm and f = 19 mm, we find very small deviations from the initial TCE values when moving along the Y axis. This indicates that there is substantial tolerance for misalignment along the Y axis during grating writing. We expect such behavior as the depth of focus for those lenses is quite large compared to the dimensions of the PCF, as described in Section 2 and as shown in Figs. 2(c) and 2(d).

For shorter focal length lenses (f = 10 mm and f = 12 mm), we find that the optimal position for efficient coupling is not at $\Delta Y = 0$ µm, but that the PCF needs to be translated by around 15 µm further from the focus of the beam to obtain the best writing conditions. Even more, at this position the TCE of the f = 10 mm lens is as high as 0.6, and almost reaches the peak values of the longer focal length lenses. Short focal lenses feature a lower tolerance for vertical positioning, which is again as expected given the shorter depth of focus, see Figs. 2(a) and 2(b).

Figures 6(a) and 6(b) show the intensity distribution in the PCF holey cladding during grating writing. The first image shows the case for $\Delta Y = 0$ µm, while the second shows the case for $\Delta Y = -15$ µm. We clearly see that, when the PCF is translated such that the Gaussian beam waist is close to the edge of the microstructure as shown in Fig. 6(b), transverse beam guiding in between holes towards the core region is more efficient, yielding notably higher intensity values in the core region and lower amounts of scattered light.

Optics EXPRESS

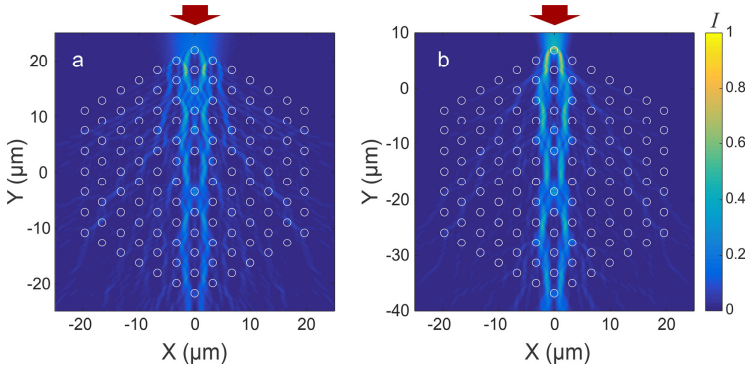

Fig. 6. Intensity distribution in the PCF microstructure with a lens with focal length f = 10 mm when the fiber is translated along the Y axis by a) ΔY = 0 μm and b) ΔY = –15 μm.

We repeated the calculations for the rotational dependence for this new 'optimal' position of the PCF. The results are depicted in Fig. 7. For ΔY = –15 μm, the rotational dependence is much more pronounced compared to the case when ΔY = 0 μm. The curve resembles that of the lens with f = 30 mm shown in Fig. 4 and displays a similar magnitude of the oscillation and of the maximum TCE value. Hence, an increased TCE appears to lead to an increased rotational dependence.

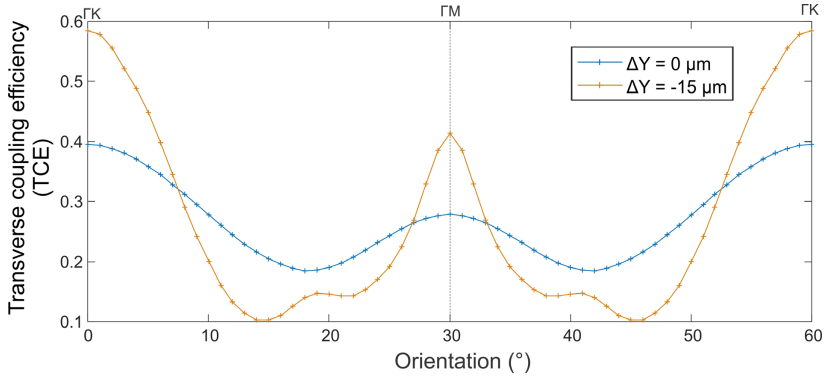

Fig. 7. TCE dependence on the PCF angular orientation for vertical translations of the focus ΔY = 0 μm and ΔY = –15 μm relative to the center of the core region.

5. Phase mask grating inscription experiments

From the simulation results obtained in the previous sections, we conclude that phase mask inscription with a cylindrical lens with shorter focal length (at least down to f = 10 mm) should be comparable with that using a lens with f = 30 mm, provided the fiber is accurately vertically translated to an optimal position which does not coincide with that of the actual focus.

Given this conclusion, we proceeded to actual femtosecond pulse grating inscription by slightly modifying the phase mask setup assembled for writing gratings in standard step-index fibers. The only supplements were fiber rotation stages added to control the relative orientation of the PCF.

The phase mask setup, as shown schematically in Fig. 1 uses an acylindrical lens (f = 10 mm) to minimize geometrical aberrations. For the laser source we used a commercial Yb:KGW ultrafast regenerative amplifier system Pharos 6W (Light Conversion) at 1030 nm wavelength with 190 fs duration pulses and a repetition rate of 100 Hz. The output beam diameter of the laser used for grating writing was 4 mm, which defines the maximum grating length. To the best of our knowledge, phase mask IR femtosecond grating inscription in PCF

Optics EXPRESS

with such a short focal length lens was never performed before. The same goes for the wavelength of 1030 nm used with such phase mask writing method, as the photon energy of the laser here is lower than that of the more traditional 800 nm emitted by the traditionally used Ti:Sapphire laser.

We used a high accuracy alignment mechanism to translate the PCF along the X and Y coordinates in the cross-sectional plane. The fiber itself was placed on two rotation stages from each side to control the angular orientation of the PCF. To enable active alignment of the writing beam in the PCF cross-section, we first illuminated the stripped PCF with low power pulses and we monitored the luminescence signal from the germanium doped core (around 420 nm, as described in [31]) using a commercial spectrometer from Ocean Optics. We always used a short fiber to connect to the spectrometer with minor absorption losses.

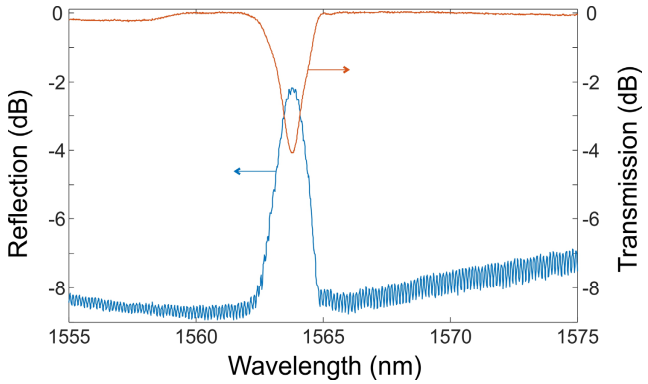

Fig. 8. Transmission and reflection spectrum of the femtosecond pulsed laser-based grating inscribed in the hexagonal lattice PCF using phase mask setup and cylindrical lens with f = 10 mm.

After 4 to 5 attempts with different samples we identified the necessary conditions (laser power, luminescence intensity, etc.) and we successfully inscribed relatively strong FBGs in the hexagonal lattice PCF using a laser power of 450 mW with a total illumination time of around 4 seconds only. Prior to the inscription, we optimized the orientation of the PCF by rotating it with the increments of 10° relative to the initial random position (the absolute angular orientation was not controlled). Once a strong luminescence was observed, we increased the laser power to write the grating. The reflection and transmission spectra of the second order grating are shown in Fig. 8, revealing a transmission dip of almost 4 dB. Note that no transverse scanning was carried out. We limited the illumination time to 4 seconds to avoid possible degradation of the reflection and transmission spectrum, which we observed in our previous writing attempts.

We close this section by emphasizing the importance of controlling the laser power during grating writing: At lower powers we did not observed any grating growth, which is a consequence of the non-linear nature of the index change. Increasing the laser power above a certain level resulted in the appearance of multi-peak structures near the resonance wavelength, accompanied with the decrease of the transmission level in the spectral range around 1550 nm. Note that this phenomenon is specific to PCFs and not observed in in standard step-index fibers. A likely reason for that could be the structural modifications at the air/silica interfaces due to the highly non-linear light-matter interactions. This was also indicated by strong scattering at the location of the grating when coupling white light into the fiber.

6. Conclusions

We presented a detailed numerical study and the experimental demonstration of IR femtosecond pulse grating in a hexagonal lattice PCF using a phase mask technique and a

Optics EXPRESS

short focal length cylindrical lens. It is the first time that a phase mask technique-based FBG is written in a PCF with a 1030 nm laser.

We first numerically studied the peculiarities of IR femtosecond grating inscription in a hexagonal lattice PCF using a phase mask method with cylindrical lenses with different focal lengths f = 10 mm, 12 mm, 19 mm and 30 mm. More specifically, we analyzed the dependence of the transverse coupling efficiency (TCE) on the PCF's angular orientation when the grating writing beam is focused to the center of the fiber and we found that shorter focal length lenses may lead to lower rotational dependence. At the same time, maximal TCE values were larger for cylindrical lenses with longer focal lengths. We then studied the effect of translating the optical fiber along the two principal axes in the cross-sectional plane. We have shown that for shorter focal length lenses, the optimal position of the PCF differs from that of a step-index fiber. For a cylindrical lens with a focal length as short as 10 mm, the PCF should be translated down by 15 μm, further away from the Gaussian beam waist and phase mask to obtain optimal coupling. In this position, the beam is focused almost at the edge of the microstructure and the TCE is substantially larger, achieving values identical to those of a lens with f = 30 mm. This goes at the expense of an increased rotational dependence.

In the experimental part of the work, we succeeded writing femtosecond pulsed laser-based FBGs in the same hexagonal lattice PCF as considered in the numerical study. The PCF was positioned on high accuracy translation stages in order to carefully align the focal position in the cross-sectional plane. The PCF's angular orientation was controlled as well using rotation stages. At the optimal laser power, we managed to inscribe a second order FBG in only 4 seconds with a –2dB reflection strength.

These results pave the way towards more efficient IR femtosecond grating inscription with phase masks in standard hexagonal lattice PCFs and allow envisaging through-coating grating writing in such fibers, which we will address in future work.

Funding

Research Foundation-Flanders (FWO) (G0F6218N-EOS ID 30467715, postdoctoral fellowship 12P1717N); European Cooperation in Science and Technology (COST) (MP1401).

Acknowledgments

The authors of Vrije Universiteit Brussel also wish to acknowledge VUB's Methusalem Foundation as well as the Hercules Foundation–Flanders.